

Accepted Manuscript

Synthesis and evaluation of N-(benzofuran-5-yl) aromaticsulfonamide derivatives as novel HIF-1 inhibitors that possess anti-angiogenic potential

Jinlian Wei, Yingrui Yang, Yali Li, Xiaofei Mo, Xiaoke Guo, Xiaojin Zhang, Xiaoli Xu, Zhengyu Jiang, Qidong You

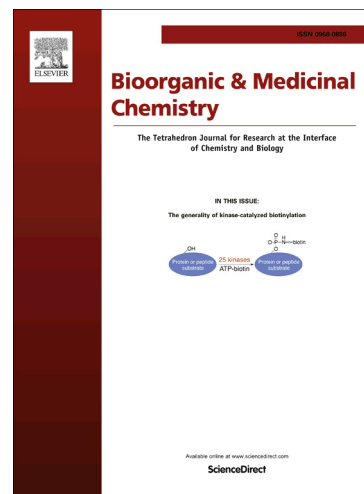
PII: S0968-0896(16)30444-8
DOI: <http://dx.doi.org/10.1016/j.bmc.2016.06.021>
Reference: BMC 13077

To appear in: *Bioorganic & Medicinal Chemistry*

Received Date: 2 May 2016
Revised Date: 8 June 2016
Accepted Date: 11 June 2016

Please cite this article as: Wei, J., Yang, Y., Li, Y., Mo, X., Guo, X., Zhang, X., Xu, X., Jiang, Z., You, Q., Synthesis and evaluation of N-(benzofuran-5-yl) aromaticsulfonamide derivatives as novel HIF-1 inhibitors that possess anti-angiogenic potential, *Bioorganic & Medicinal Chemistry* (2016), doi: <http://dx.doi.org/10.1016/j.bmc.2016.06.021>

This is a PDF file of an unedited manuscript that has been accepted for publication. As a service to our customers we are providing this early version of the manuscript. The manuscript will undergo copyediting, typesetting, and review of the resulting proof before it is published in its final form. Please note that during the production process errors may be discovered which could affect the content, and all legal disclaimers that apply to the journal pertain.



Graphical Abstract

To create your abstract, type over the instructions in the template box below.
 Fonts or abstract dimensions should not be changed or altered.

Leave this area blank for abstract info.

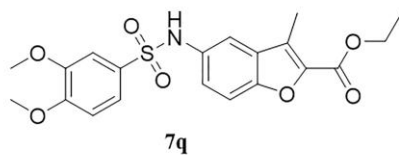
Synthesis and evaluation of N-(benzofuran-5-yl) aromaticsulfonamide derivatives as novel HIF-1 inhibitors that possess anti-angiogenic potential

Jinlian Wei,^{a,b} Yingrui Yang,^{a,b} Yali Li,^{a,b} Xiaofei Mo,^{a,b} Xiaoke Guo,^{a,b} Xiaojin Zhang,^{a,b,c} Xiaoli Xu,^{a,b} Zhengyu Jiang,^{a,b} and Qidong You,^{a,b,*}

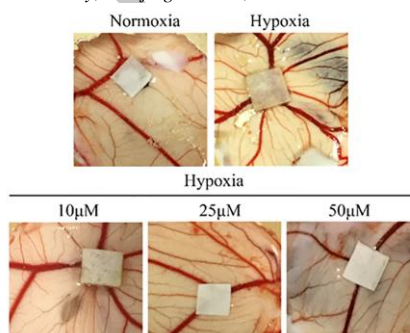
^aState Key Laboratory of Natural Medicines and Jiangsu Key Laboratory of Drug Design and Optimization, China Pharmaceutical University, Nanjing 210009, China

^bDepartment of Medicinal Chemistry, School of Pharmacy, China Pharmaceutical University, Nanjing 210009, China

^cDepartment of Organic Chemistry, School of Science, China Pharmaceutical University, Nanjing 210009, China



MCF-7-HRE (IC₅₀): 12.5 ± 0.7 μM





Synthesis and evaluation of N-(benzofuran-5-yl) aromaticsulfonamide derivatives as novel HIF-1 inhibitors that possess anti-angiogenic potential

Jinlian Wei,^{a,b} Yingrui Yang,^{a,b} Yali Li,^{a,b} Xiaofei Mo,^{a,b} Xiaoke Guo,^{a,b} Xiaojin Zhang,^{a,b,c} Xiaoli Xu,^{a,b} Zhengyu Jiang,^{a,b} and Qidong You,^{a,b,*}

^aState Key Laboratory of Natural Medicines, and Jiangsu Key Laboratory of Drug Design and Optimization, China Pharmaceutical University, Nanjing 210009, China

^bDepartment of Medicinal Chemistry, School of Pharmacy, China Pharmaceutical University, Nanjing 210009, China

^cDepartment of Organic Chemistry, School of Science, China Pharmaceutical University, Nanjing 210009, China

ARTICLE INFO

Article history:

Received

Received in revised form

Accepted

Available online

Keywords:

N-(benzofuran-5-yl) aromaticsulfonamide derivatives

HIF-1

Transcriptional activity

Migration

Anti-angiogenesis

ABSTRACT

Hypoxia-inducible factor-1 (HIF-1) as a key mediator in tumor metastasis, angiogenesis, and poor patient prognosis has been recognized as an important cancer drug target. A novel series of N-(benzofuran-5-yl) aromaticsulfonamide derivatives were synthesized and evaluated as HIF-1 inhibitor. Among these compounds, **7q** exhibited specific inhibitory effects on HIF-1 by downregulating the expression of HIF-1 α under hypoxic conditions. It inhibited the HIF-1 transcriptional activity ($IC_{50} = 12.5 \pm 0.7 \mu M$) and secretion of VEGF ($IC_{50} = 18.8 \mu M$) in MCF-7 cells. Meanwhile, it also significantly suppressed hypoxia-induced migration of HUVEC cells in nontoxic concentrations. Additionally, tube formation assay demonstrated its anti-angiogenesis activity. Finally, the *in vivo* study indicated that compound **7q** could retard angiogenesis in CAM model. These findings supported the HIF-1 inhibitory effect and anti-angiogenic potential of this class of compounds as HIF-1 inhibitor.

2016 Elsevier Ltd. All rights reserved.

1. Introduction

There is an increasing number of focuses on transcription factors which are found to be associated with various cellular progress.¹ Hypoxia is a hallmark of many malignant tumors and is regulated by hypoxia-inducible factor-1 (HIF-1), a transcription factor orchestrating the expression of many genes that code for proteins involved in angiogenesis, glucose metabolism, cell proliferation and metastasis.² Overexpression of HIF-1 in tumor cells is closely connected with the more resistant to radio- and chemo-therapies, the increased risk of metastasis, the more aggressive phenotype and the strengthened immune suppression.³ Consequently, inhibition of HIF-1 pathway may contribute to specific cancer therapies, especially those cancers tightly correlated to hypoxia.^{4,5}

HIF-1 is a bHLH-PAS (basic-helix-loop-helix-PER-ARNT-SIM) heterodimer consisting of two subunits: HIF-1 α and HIF-1 β (also known as the aryl hydrocarbon receptor nuclear translocator, ARNT).⁶ The level of HIF-1 α is O₂-dependent while HIF-1 β is constitutively expressed.⁷ Under normal oxygen conditions, HIF-1 α is hydroxylated by prolyl hydroxylase (PHD) at residues of Pro402 and Pro564, and is subjected to proteasome degradation through the following recognition of von Hippel-Lindau (pVHL).⁸⁻¹⁰ Besides, Asn803 of HIF-1 α C-terminal transactivation domain (C-TAD) is hydroxylated by the factor-

inhibiting HIF (FIH), whose catalysis is also O₂-dependent.¹¹ However, under hypoxic conditions, HIF-1 α is stabilized without being hydroxylated by PHD and FIH, translocates into the nuclear and heterodimerizes with HIF-1 β , and then recruits transcriptional coactivator proteins.¹²⁻¹³ The complex HIF-1 α /HIF-1 β /coactivator protein initiates an adaptive hypoxic transcription of a vast variety of target genes through binding with their hypoxia-responsive elements (HREs), including those protein products that are correlated with angiogenesis, metabolic reprogramming, invasion and metastasis of cancer cells.² It has been well established that HIF-1 α plays a significant role in multiple processes of cancer development, therefore, it is recognized as a promising target for cancer therapy.

Among diverse cancer types, breast cancer stands out because of its increasing incidence rate and high mortality worldwide.¹⁴ Breast cancer has become the second leading cause of death in female patients only after lung cancer.¹⁵ Evidences supported that HIF-1 was correlated with poor prognosis in human breast cancer due to the high metastasis and HIF-1 expression.^{2,16} It has been reported that expression of HIF-1 target genes was increased in the triple-negative breast cancer.¹⁷⁻¹⁸ Breast cancer cell lines, such as MCF-7 and MDA-MB-231, have been used as classical tools for HIF-1 pathway research.¹⁹ So far, several HIF-1 inhibitors have been discovered, such as

* Corresponding author. Tel. / fax: +86-25-8327-1216; e-mail: youqd@163.com

topotecan,²⁰ bortezomib,²¹ YC-1,²² and PX-478 (Fig. 1).²³ Topotecan and bortezomib have been approved for marketing,²⁴ ²⁵ YC-1 and PX-478 are undergoing clinical trials on patients expressing high levels of HIF-1 α in their tumors.²⁶⁻²⁷ However, the chemotype of HIF-1 α inhibitor is still limited, discovery of new HIF-1 α inhibitor with better efficiency is still an important task for medicinal chemists.

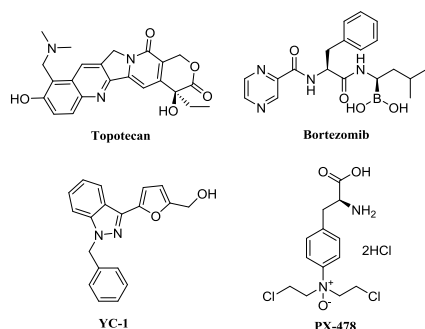


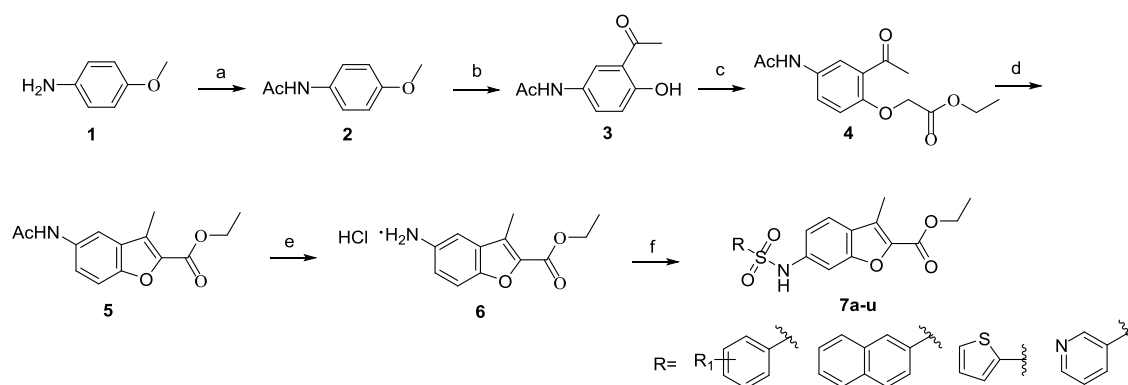
Figure 1. Structures of representative HIF-1 inhibitors.

We have carried out a screening of our in-house compound collection for searching compounds that can inhibit HIF-1 α transcriptional activity in MCF-7 cells under hypoxic condition by a cell-based HRE reporter assay. Compound **7a**, with N-(benzofuran-5-yl) benzenesulfonamide core, showed inhibitory effect on HIF-1 α transcriptional activity. Considering this was a new chemotype for HIF-1 α inhibition, it was then recognized as the starting compound for further structural optimization.

2. Results and discussion

2.1 Chemistry

Some novel N-(benzofuran-5-yl) aromaticsulfonamide derivatives were designed by changing the substituents on other benzene-ring or replacing the benzene-ring with naphthyl, thienyl or pyridyl in order to investigate its preliminary structure-activity of HIF-1 inhibition. The target compounds were synthesized as shown in **Scheme 1**. 4-methoxyaniline (**1**) was treated with Ac₂O, and the protected aniline **2** was converted to N-(3-acetyl-4-hydroxyphenyl) acetamide **3** by Friedel-Crafts acylation. **4** was formatted through nucleophilic substitution of **3** and BrCH₂COOEt under alkaline conditions. Furan ring **5** was obtained through a cyclization *via* microwave. Deacetylation of **5** in the acidic condition generated intermediate **6**. The final products of N-(benzofuran-5-yl) aromaticsulfonamides **7a-u** were generated through condensation reactions of **6** with different sulfonyl chloride.



Scheme 1. Synthesis of N-(benzofuran-5-yl) aromaticsulfonamide **7a-u**. Reagents and conditions: (a) DCM, Ac₂O, N₂, reflux, 2 h,

2.2 Pharmacology

2.2.1. N-(benzofuran-5-yl) aromaticsulfonamide derivatives inhibit HIF-1 transcriptional activity

The N-(benzofuran-5-yl) aromaticsulfonamide derivatives **7a-u** were tested for their inhibitory effect on HIF-1 transcriptional activity in MCF-7 cells under hypoxic conditions (1% O₂) using dual luciferase reporter gene assay (**Table 1**). **PX-478** was used as a positive control. Different chemical groups, including methyl, chloro, bromo, trifluoromethyl, tert-butyl and nitro (**7a~7p**) were introduced onto the benzene ring of benzenesulfonamide. Generally, these groups did not affect the HRE activity obviously, indicating that mono-substitution was not favorable to the HIF-1 inhibition. Meanwhile, compounds with *ortho*-substituted phenyl (**7c**, **7f**, **7i**, **7l**, **7o**) exhibited better HIF-1 inhibitory potency, compared to the corresponding *meta*-(**7b**, **7e**, **7h**, **7k**, **7n**) and *para*-(**7a**, **7d**, **7g**, **7j**, **7m**) ones (**Table 1**). There was an enhancement in HIF-1 inhibition when 3,4-dimethoxyphenyl (**7q**) was introduced to the structure of N-(benzofuran-5-yl) sulfonamide, with an IC₅₀ value of 12.5 ± 0.7 μM. 2,5-disubstituted methoxyphenyl (**7r**) was also introduced, with an IC₅₀ value of 15.7 ± 1.6 μM, suggesting that dimethoxyphenyl might be better options. To examine the importance of the benzenesulfonamide moiety, the benzene-ring was replaced by other rings including 2-naphthyl (**7s**), 2-thienyl (**7t**) and 3-pyridyl (**7u**). **7s** maintained its activity in HRE assays, consistent with that of compound **7p**. It indicated larger and more hydrophobic groups were preferred at benzenesulfonamide moiety. On the contrary, substitution with aromatic heterocycles reduced the HIF-1 transcriptional activity, suggesting that polar groups were popular in further optimization. The antiproliferative activities of **7a-u** toward human breast cancer cell lines were weaker than their HIF-1 transcription inhibitory activities (**Table 1**), revealing that N-(benzofuran-5-yl) aromaticsulfonamide derivatives **7a-u** suppressed HIF-1 transcriptional activity without cytotoxicity. The results were the same with those previously reported HIF-1 inhibitors, such as YC-1 and PX-478, which inhibited HIF-1 transcriptional activity at lower concentrations and blocked tumor cell proliferation at much higher concentrations.²⁶⁻²⁷ It is probably due to the hypoxia microenvironment itself, inhibiting HIF-1 pathway could primarily affect progresses of angiogenesis, migration and invasion, while the tumor growth could take place later.² Together, compound **7q** with the best HIF-1 inhibitory effect (IC₅₀ = 12.5 ± 0.7 μM, slightly more potent than positive control **PX-478**, IC₅₀ = 20.2 ± 4.4 μM) was selected for further biological evaluation.

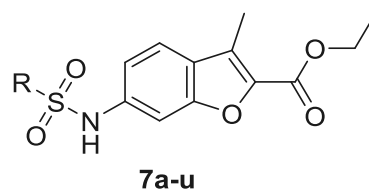
94%; (b) DCM, AcCl₂, AlCl₃, reflux, 12 h, 78%; (c) DMF, BrCH₂COOEt, K₂CO₃, KI, 80 °C, 4 h, 87%; (d) DMF, K₂CO₃, microwave, 145 °C, 7 min, 59%; (e) EtOH, 3M HCl, N₂, reflux, 6 h, 71%; (f) DCM, RSO₂Cl, pyridine, *rt.*, 12 h, 56% ~ 82%.

2.2.2. 7q suppresses HIF-1 α and VEGF

The levels of HIF-1 mainly depended on the regulation of HIF-1 α , which is oxygen sensitive. Many HIF-1 α inhibitors have been developed and their mechanisms of action have been fully demonstrated, such as to decrease HIF-1 α mRNA levels,²⁸ to inhibit HIF-1 α protein synthesis,²⁹ to promote HIF-1 α degradation,³⁰ to block HIF-1 α binding to DNA,³¹ and to suppress HIF-1 α transcriptional activity.³² In order to explore the

mechanism of 7q, we first examined the effects of 7q on the expression of HIF-1 α in hypoxia. As shown by the data, the levels of HIF-1 α mRNA were unchanged without 7q treatment in both normoxia and hypoxia, but were decreased after the treatment of 7q in hypoxia in a dose-dependent manner (Fig. 2a). Compared with little expression in normoxia, HIF-1 α protein level was greatly boosted under hypoxia,³³⁻³⁴ which can be reduced by 7q in a concentration-dependent manner in MCF-7 cells (Fig. 2b-c).

Table 1. *In vitro* inhibition of HIF-1 α transcriptional activity in cell-based HRE reporter assay under hypoxia conditions and cytotoxicity under hypoxia conditions.



ID	R	HRE-Luc IC ₅₀ (μM) ^a	Antiproliferative activity IC ₅₀ (μM) ^b		
			MCF-7	MDA-MB-231	MDA-MB-468
7a	4-methylphenyl	45.4 ± 8.3	53.9 ± 7.7	25.2 ± 1.8	24.0 ± 1.2
7b	3- methylphenyl	32.7 ± 2.8	101.2 ± 9.9	29.5 ± 1.5	25.3 ± 5.2
7c	2- methylphenyl	19.4 ± 1.8	105.2 ± 8.2	89.2 ± 7.0	53.4 ± 2.8
7d	4-chlorophenyl	50.0 ± 5.8	81.2 ± 5.4	53.9 ± 2.1	44.0 ± 1.0
7e	3- chlorophenyl	36.6 ± 0.5	83.9 ± 8.1	57.3 ± 1.0	53.7 ± 4.7
7f	2- chlorophenyl	20.8 ± 2.1	>200	>200	137.4 ± 2.2
7g	4-bromophenyl	29.9 ± 3.3	56.5 ± 2.3	31.1 ± 4.0	26.4 ± 3.6
7h	3- bromophenyl	25.6 ± 2.8	57.0 ± 0.4	33.7 ± 3.4	30.7 ± 1.9
7i	2- bromophenyl	19.9 ± 1.6	185.4 ± 23.6	178.7 ± 9.5	138.4 ± 21.3
7j	4-(trifluoromethyl)phenyl	41.7 ± 3.9	48.7 ± 1.4	24.3 ± 4.2	27.2 ± 3.6
7k	3-(trifluoromethyl)phenyl	36.3 ± 5.8	51.4 ± 0.2	30.2 ± 2.8	28.9 ± 4.2
7l	2-(trifluoromethyl)phenyl	16.5 ± 2.0	93.9 ± 0.9	82.4 ± 5.6	74.9 ± 3.2
7m	4-nitrophenyl	36.2 ± 5.1	69.6 ± 7.9	33.1 ± 1.6	24.0 ± 3.8
7n	3- nitrophenyl	29.4 ± 2.5	74.8 ± 3.5	59.9 ± 8.7	30.1 ± 4.1
7o	2- nitrophenyl	24.4 ± 3.7	156.9 ± 10.1	80.4 ± 7.3	96.9 ± 6.2
7p	4-tert-butylphenyl	27.1 ± 1.9	22.1 ± 2.3	22.4 ± 1.7	8.1 ± 1.1
7q	3,4-dimethoxyphenyl	12.5 ± 0.7	52.0 ± 3.8	35.4 ± 3.1	20.5 ± 3.0
7r	2,5-dimethoxyphenyl	15.5 ± 2.6	52.3 ± 7.2	26.7 ± 2.7	20.7 ± 2.1
7s	2-naphthyl	22.6 ± 3.2	20.8 ± 3.1	21.6 ± 1.6	15.7 ± 0.9
7t	2-thienyl	45.4 ± 4.5	92.3 ± 10.2	44.1 ± 1.3	34.3 ± 4.0
7u	3-pyridyl	34.1 ± 2.9	>200	140.8 ± 12.7	62.9 ± 3.9
PX-478		20.2 ± 4.4	19.7 ± 1.1	62.8 ± 9.0	45.1 ± 3.6

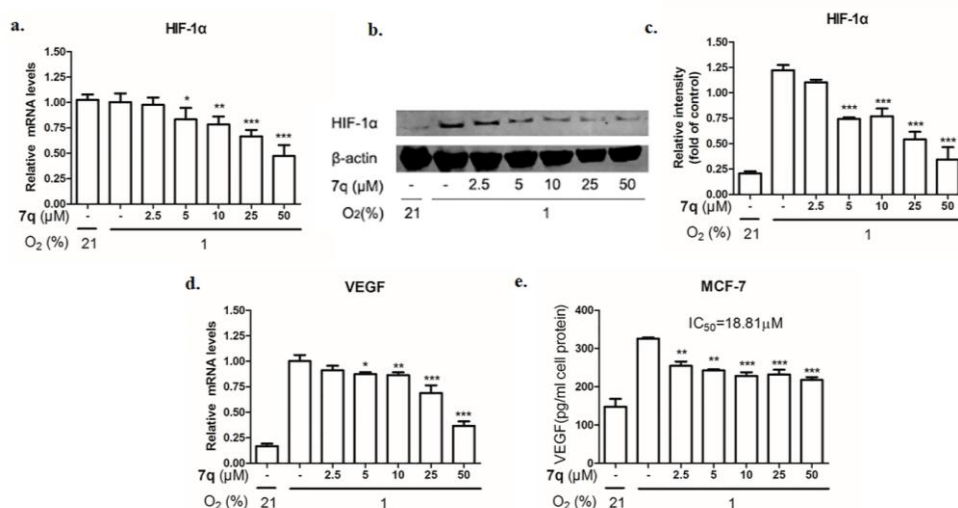


Figure 2. The effects of compound **7q** on the expression levels of HIF-1 α and VEGF in MCF-7 cells. (a) HIF-1 α mRNA was measured by RT-PCR analyses in MCF-7 cells after **7q** treatment for 24h under normoxia or hypoxia conditions. β -actin was used as internal control. Bars are the mean \pm SD (n = 3). Statistical significance: *: P < 0.05, **: P < 0.01, and ***: P < 0.001 versus hypoxia control. (b) HIF-1 α protein expression was detected by immunoblot analysis with the specific antibody. β -actin was used as an internal control. (c) For quantity of (b), images were analyzed using ImageJ software. Bars are the mean \pm SD (n = 3). The comparisons were made relative to hypoxia alone group, and the different levels of significance were indicated as *P < 0.05 and **P < 0.01 and ***: P < 0.001. (d) mRNA levels of VEGF was detected by RT-PCR. β -actin was used as an internal control. Bars are the mean \pm SD (n = 3). Statistical significance: *: P < 0.05, **: P < 0.01, and ***: P < 0.001 versus hypoxia control. (e) The secretion of VEGF protein in MCF-7 cells was obviously suppressed by **7q**. The cells were incubated for 24 h with or without treatment. Bars are the mean \pm SD (n = 3). Statistical significance: **: P < 0.01, and ***: P < 0.001 versus hypoxia control.

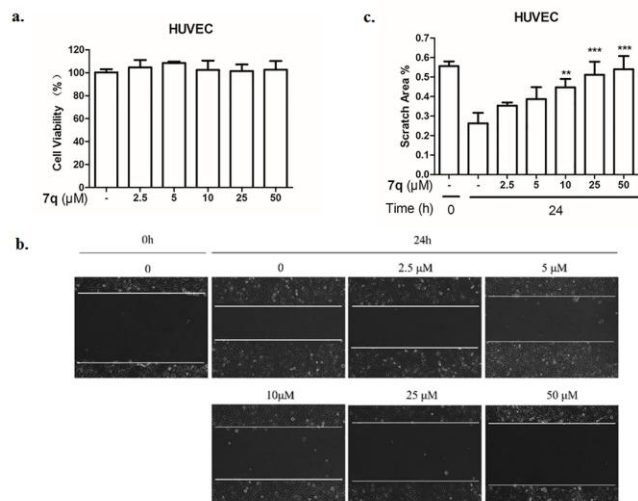


Figure 3. The effects of **7q** on hypoxia-induced migration on HUVEC cells. (a) The cell survival of HUVECs with different concentrations of **7q** treatment (24 h) was detected using MTT assay. All error bars are the mean \pm SD (n = 3). (b) HUVEC cells migration was measured by wound healing assay. The cells were treated **7q** at different concentrations. The straight lines indicate the scratched wound gaps. (c) For quantity of (b), images were analyzed using ImageJ software. Bars are the mean \pm SD (n = 3). The comparisons were made relative to the control group of 24 h, and the different levels of significance were indicated as **: P < 0.01 and ***: P < 0.001.

During hypoxia, HIF-1 α accumulates and translocates into nuclei where it activates the transcription of downstream genes, such as VEGF. Thus, in order to confirm the effect of **7q** on HIF-1 activation, further studies were focused on the changes of the mRNA and protein levels of VEGF after **7q** treatment. As shown by the data, both mRNA levels of VEGF were remarkably suppressed in a dose-dependent fashion after **7q** treatment (**Fig. 2d**), indicating that the transcriptional activation of HIF-1 α was inhibited. The effect of compound **7q** on hypoxia-induced VEGF secretion was then measured using ELISA (enzyme-linked immunosorbent assay) method. Data confirmed that **7q** significantly inhibited the hypoxia-induced secretion of VEGF in MCF-7 cells in a concentration-dependent manner, and the IC₅₀ value was calculated as 18.8 μ M (**Fig. 2e**). Taken together, these findings suggested that **7q** suppressed HIF-1 transcriptional activity affecting both HIF-1 α mRNA levels and HIF-1 α protein accumulation, and blocked the expression of its downstream target gene VEGF.

2.2.3. **7q** reduces hypoxia-induced cell migration

It is well known that HIF-1 activation can promote cancer cell migration and angiogenesis through activating transcription of specific genes, such as VEGF.³⁵ To explore the HIF-1 related

biological of **7q**, we subsequently performed wound healing migration assays to determine **7q** on HUVEC migration. To avoid direct cytotoxic effects, the cell viability of HUVEC was assessed by MTT at first. As shown by the data (**Fig. 3a**), **7q** could not induce obvious cytotoxicity for HUVEC cells. In the next wound healing assay, the number of migrating HUVEC cells decreased in a concentration-dependent manner (**Fig. 3b-c**). These results suggested that nontoxic doses of **7q** possess anti-migratory potential.

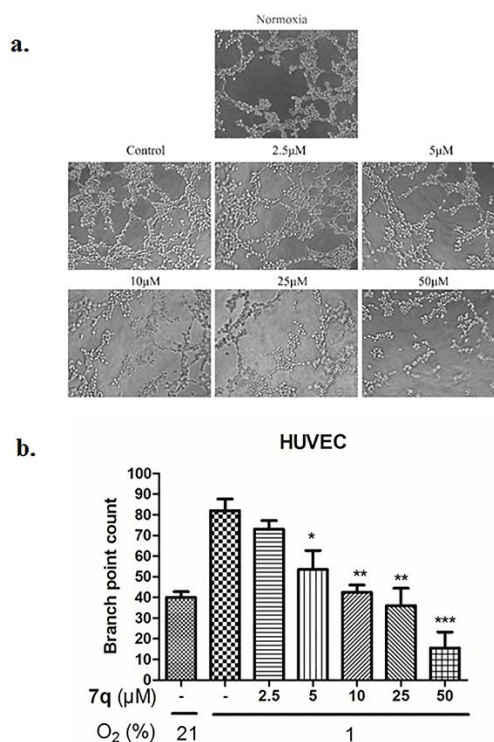


Figure 4. Effect of **7q** on the hypoxia-enhanced HUVECs tube formation. (a) HUVECs tube formation was measured after **7q** treatment for 24 h. The experiments were performed as described in capillary-like tube formation. (b) Quantification of the effect of **7q** on tube formation is shown in column diagram. Bars are the mean \pm SD (n = 3). Statistical significance: *: P < 0.05, **: P < 0.01, and ***: P < 0.001 versus hypoxia control.

2.2.4. **7q** inhibits hypoxia-induced tube formation

Although the process of angiogenesis is very complex, tube formation of endothelial cells is one of the key steps.³⁶ Thus, we settled down to investigate how **7q** affected tube formation using two dimensional Matrigel assay. As shown in **Fig. 4a**, tube-like structures were robustly formed under hypoxia conditions compared with normoxia conditions. After **7q** treatment, the formation of tubular structures were greatly reduced in a

concentration-dependent manner (Fig. 4b). These results revealed that 7q can inhibit angiogenesis *in vitro*.

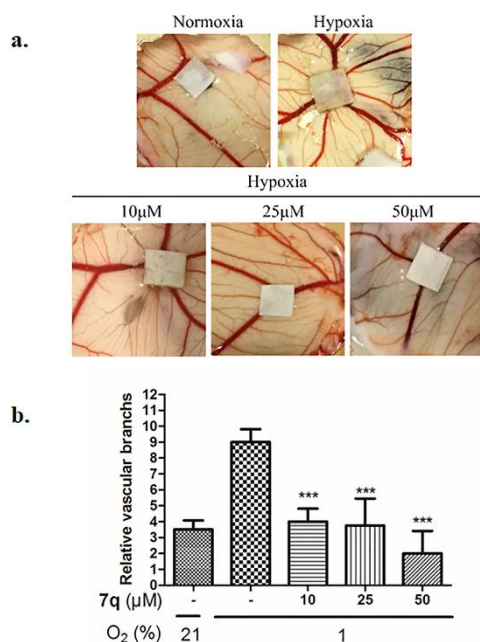


Figure 5. Effect of **7q** on the hypoxia-enhanced angiogenesis *in vivo* using CAM assay. (a) Different concentrations of **7q** were placed on the exposed CAM for 3 days to inhibit angiogenesis. (b) Quantification of the effect of **7q** on tube formation is shown in column diagram. Bars are the mean \pm SD ($n = 3$). Statistical significance: ***: $P < 0.001$ versus hypoxia control.

2.2.5. 7q inhibits hypoxia-induced angiogenesis *in vivo*

To assess the anti-angiogenesis activity of **7q**, different angiogenesis models were employed. Here, we additionally performed the Chicken chorioallantoic membrane (CAM) assay to verify the anti-angiogenesis capacity of **7q**. From this model, we focused on the process of new blood vessel formation and vessel responses to **7q**. From the data in Fig. 5a, more and thicker new blood vessels were formed in response to hypoxic stimulus. When different concentrations of **7q** (10, 25 and 50 μM) was used, the quantity of vessels was reduced, and the thick ones vanished. It indicated that **7q** inhibited the *in vivo* angiogenesis in a concentration-dependent manner (Fig. 5b).

3. Conclusion

HIF-1 is a promising target of cancer therapy. Based on this target, numbers of chemical inhibitors have been disclosed. In the current study, we identified **7a** and developed its derivatives containing N-(benzofuran-5-yl) aromaticsulfonamide core as HIF-1 inhibitors. Among all the compounds, **7q** showed the best inhibitory effect against HIF-1 activity ($\text{IC}_{50} = 12.5 \pm 0.7 \mu\text{M}$). Western blot assay and RT-PCR analysis indicated that **7q** downregulated the expression of HIF-1 α in hypoxia, and further blocked its transcription activation on VEGF both in mRNA levels and protein levels ($\text{IC}_{50} = 18.8 \mu\text{M}$). Because VEGF is associated with cell angiogenesis and migration, the suppressed functionality of VEGF by **7q** treatment led to decreased HUVEC migration and tube formation. In addition, **7q** exhibited significant blockade in angiogenesis in CAM model. In conclusion, a new chemotype as HIF-1 inhibitor, N-(benzofuran-

5-yl) aromaticsulfonamide was identified and verified. The best compound **7q**, would provide a promising lead for further optimization in discovering new HIF-1 inhibitors.

4. Experimental section

4.1 Chemistry

Unless stated otherwise, all reagents and solvents were used as received from commercial suppliers. Reactions in microwave reactors were performed by single-node heating in an Initiator (Biotage). ¹H NMR and ¹³C NMR spectra were recorded with a Bruker Avance 300 MHz spectrometer at 300 MHz and 75 MHz, respectively, at 303 K using TMS as an internal standard. High resolution mass spectra (HRMS) were recorded on a Water Q-ToF micro mass spectrometer. HPLC analysis for reaction monitoring and purity determination was performed on an Agilent1100 LC system by the standard method on an Amethyst C18-P column (4.6 \times 150 mm, 5 μm , Merck); $\lambda = 254 \text{ nm}$; mobile phase: A (acetonitrile)/B (H_2O), 80:20 v/v.

4.1.1. Synthesis of N-(4-methoxyphenyl) acetamide (2)

Acetic anhydride (16.58 g, 162.40 mmol) was slowly dripped into a stirred solution of 4-methoxyaniline (**1**) (10 g, 81.20 mmol) in CH_2Cl_2 (120 mL) using dropping funnel. After the dripping of acetic anhydride, the reaction mixture was purged with N_2 gas and stirred at 30 $^\circ\text{C}$ for 2 h, and then the mixture was evaporated to give silver-white crude product 12.60 g (76.27 mmol, 94%). ¹H NMR (300 MHz, $\text{DMSO-}d_6$): δ 9.72 (s, 1H), 7.48 – 7.45 (m, 2H), 7.21 – 6.70 (m, 2H), 3.98 (s, 3H), 1.20 (s, 3H). Used directly for following reaction without further purifying.

4.1.2. Synthesis of N-(3-acetyl-4-hydroxyphenyl) acetamide (3)

The crude **2** (5.10 g, 30.87 mmol) was dissolved in dichloromethane (120 mL) with stirring and cooling, to which aluminium chloride and acetyl chloride were added quickly. Then the mixture was heated to reflux for 12h. After cooling to room temperature, the supernatant liquid of the mixture was poured into 100 mL ice-cold water, while the underlayer residue was stirred with 4% aqueous HCl for another half an hour. The precipitate was filtrated through buchner funnel and dried to give a yellow-green solid of 4.68g (24.22 mmol, 78%). ¹H NMR (300 MHz, $\text{DMSO-}d_6$): δ 11.55 (s, 1H), 9.93 (s, 1H), 8.06 (d, $J = 2.58 \text{ Hz}$, 1H), 7.65 (dd, $J = 2.6, 8.9 \text{ Hz}$, 1H), 6.91 (d, $J = 8.9 \text{ Hz}$, 1H), 2.58 (s, 3H), 2.01 (s, 3H); HRMS (ESI): calcd. For $\text{C}_{10}\text{H}_{12}\text{NO}_3$ $[\text{M}+\text{H}]^+$ 194.0812, found 194.0815.

4.1.3. Synthesis of ethyl 2-(4-acetamido-2-acetylphenoxy) acetate (4)

To a solution of N-(3-acetyl-4-hydroxyphenyl) acetamide **3** (4.68 g, 24.25 mmol) in DMF (50 mL), ethyl bromoacetate and potassium carbonate were added. The mixture was refluxed for 4h. Then the mixture was poured into water (200 mL), and the precipitate was filtered off and dried to give white solid (5.88 g, yield 87%). ¹H NMR (300 MHz, $\text{DMSO-}d_6$): δ 9.95 (s, 1H), 7.80 – 7.66 (m, 2H), 7.05 (d, $J = 8.9 \text{ Hz}$, 1H), 4.89 (s, 2H), 4.17 (q, $J = 7.1 \text{ Hz}$, 2H), 2.60 (s, 3H), 2.00 (s, 3H), 1.21 (t, $J = 7.1 \text{ Hz}$, 4H); HRMS (ESI): calcd. For $\text{C}_{14}\text{H}_{18}\text{NO}_5$ $[\text{M}+\text{H}]^+$ 280.1179, found 280.1175.

4.1.4. Synthesis of ethyl 5-acetamido-3-methylbenzofuran-2-carboxylate (5)

To a solution of ethyl 2-(4-acetamido-2-acetylphenoxy) acetate **4** (2.00 g, 7.16 mmol) in DMF (10 mL), potassium carbonate (1.48 g, 10.74 mmol) was added. The resulting mixture was heated under microwave irradiation (350W) for 7 min. The reaction mixture was then poured into water. The precipitate was filtered off and dried to obtain white solid (1.10 g, yield 59%); ¹H NMR (300 MHz, DMSO-*d*₆): δ 10.10 (s, 1H), 8.11 (d, *J* = 1.6 Hz, 1H), 7.65 – 7.46 (m, 2H), 4.34 (q, *J* = 7.1 Hz, 2H), 2.49 (s, 3H), 2.06 (s, 3H), 1.33 (t, *J* = 7.1 Hz, 3H); HRMS (ESI): calcd. For C₁₄H₁₆NO₄ [M+H]⁺ 262.1074, found 262.1072.

4.1.5. Synthesis of ethyl 5-acetamido-3-methylbenzofuran-2-carboxylate (6)

To a solution of 3M hydrochloric acid (20 mL) in ethanol (30 mL), **5** (1.00 g, 3.83 mmol) was added. The mixture was heated to reflux for 6 h with N₂ gas purging. The clear solution obtained was cooled to room temperature and condensed under reduced pressure to give a brown solid (0.69 g, yield 71 %). ¹H NMR (300 MHz, DMSO-*d*₆): δ 10.56 (brs, 2H), 7.84 – 7.71 (m, 2H), 7.56 – 7.44 (m, 1H), 4.35 (q, *J* = 7.1 Hz, 2H), 2.53 (s, 3H), 1.34 (t, *J* = 7.1 Hz, 3H); HRMS (ESI): calcd. for C₁₂H₁₄NO₃ [M+H]⁺ 220.0968, found 220.0964.

4.1.6. Synthesis of products 7a-u

4.1.6.1. Ethyl 3-methyl-5-((4-methylphenyl) sulfonamido) benzofuran-2-carboxylate (7a).

To a solution of hydrochloride of ethyl 5-amino-3-methylbenzofuran-2-carboxylate **5** (0.22 g, 0.90 mmol) in dichloromethane (30 mL) was added pyridine (0.29 g, 3.61 mmol) and 4-methyl benzenesulfonyl chloride (0.21 g, 1.08 mmol). The mixture was stirred overnight at room temperature, and the reaction mixture was washed with dilute HCl and water. The organic phase was dried over Na₂SO₄, concentrated in vacuo and purified by silica gel column chromatography to give **7a**, a white powder of (0.27 g, yield 82%). **7b-e** were synthesized in a similar way.

Compound **7a**: Yield, 82%; a white powder; ¹H NMR (300 MHz, DMSO-*d*₆): δ 10.23 (s, 1H), 7.65 – 7.57 (m, 2H), 7.54 (d, *J* = 8.9 Hz, 1H), 7.41 (d, *J* = 2.2 Hz, 1H), 7.31 (d, *J* = 8.0 Hz, 2H), 7.17 (dd, *J* = 8.9, 2.2 Hz, 1H), 4.33 (q, *J* = 7.1 Hz, 2H), 2.45 (s, 3H), 2.31 (s, 3H), 1.32 (t, *J* = 7.1 Hz, 3H); HRMS (ESI): calcd. For C₁₉H₁₉NO₅S [M+H]⁺ 374.1057, found 374.1059; HPLC (80% acetonitrile in water): t_R = 5.5 min, 99.0%.

4.1.6.2. Ethyl 3-methyl-5-((3-methylphenyl) sulfonamido) benzofuran-2-carboxylate (7b). Yield, 78%; a white powder; ¹H NMR (300 MHz, DMSO-*d*₆): δ 10.25 (s, 1H), 7.60 – 7.33 (m, 6H), 7.18 (dd, *J* = 8.9, 2.2 Hz, 1H), 4.33 (q, *J* = 7.1 Hz, 2H), 2.46 (s, 3H), 2.32 (s, 3H), 1.32 (t, *J* = 7.1 Hz, 3H); HRMS (ESI): calcd. For C₁₉H₁₉NO₅S [M+H]⁺ 374.1057, found 374.1053; HPLC (80% acetonitrile in water): t_R = 12.6 min, 97.0%.

4.1.6.3. Ethyl 3-methyl-5-((2-methylphenyl) sulfonamido) benzofuran-2-carboxylate (7c). Yield, 78%; a white powder; ¹H NMR (300 MHz, DMSO-*d*₆): δ 10.41 (s, 1H), 7.84 (d, *J* = 7.8 Hz, 1H), 7.55-7.45 (m, 2H), 7.45 – 7.25 (m, 3H), 7.18 (dd, *J* = 8.9, 2.2 Hz, 1H), 4.31 (q, *J* = 7.1 Hz, 2H), 2.58 (s, 3H), 2.42 (s, 3H),

1.31 (t, *J* = 7.1, 3H); HRMS (ESI): calcd. For C₁₉H₁₉NO₅S [M+H]⁺ 374.1057 found 374.1053; HPLC (80% acetonitrile in water): t_R = 6.0 min, 99.7%.

4.1.6.4. Ethyl 3-methyl-5-((4-chlorophenyl) sulfonamido) benzofuran-2-carboxylate (7d). Yield, 69%; a pink powder; ¹H NMR (300 MHz, DMSO-*d*₆): δ 10.40(s, 1H), 7.74-7.56 (m, 5H), 7.45 (d, *J* = 1.8 Hz, 1H), 7.18 (dd, *J* = 8.9, 2.0 Hz, 1H), 4.34 (q, *J* = 7.1 Hz, 2H), 2.46(s, 3H), 1.33 (t, *J* = 7.1 Hz, 3H); HRMS (ESI): calcd. For C₁₈H₁₆ClNO₅S [M+H]⁺ 394.0510, found 394.0525; HPLC (80% acetonitrile in water): t_R = 8.0 min, 99.9%

4.1.6.5. Ethyl 3-methyl-5-((3-chlorophenyl) sulfonamido) benzofuran-2-carboxylate (7e). Yield, 81%; a white powder; ¹H NMR (300 MHz, DMSO-*d*₆) δ 10.41 (s, 1H), 7.77 – 7.50 (m, 5H), 7.47 – 7.37 (m, 1H), 7.22 – 7.09 (m, 1H), 4.33 (q, *J* = 7.1 Hz, 2H), 2.46 (s, 3H), 1.32 (t, *J* = 7.1 Hz, 3H); HRMS (ESI): calcd. For C₁₈H₁₆ClNO₅S [M+H]⁺ 394.0510, found 394.0504; HPLC (80% acetonitrile in water): t_R = 6.4 min, 98.6%.

4.1.6.6. Ethyl 3-methyl-5-((2-chlorophenyl) sulfonamido) benzofuran-2-carboxylate (7f). Yield, 80%; a white powder; ¹H NMR (300 MHz, DMSO-*d*₆) δ 10.66 (s, 1H), 8.06 – 7.96 (m, 1H), 7.69 – 7.37 (m, 5H), 7.23 (dd, *J* = 8.9, 2.2 Hz, 1H), 4.32 (q, *J* = 7.10 Hz, 2H), 2.43 (s, 3H), 1.31 (t, *J* = 7.1 Hz, 3H); HRMS (ESI): calcd. For C₁₈H₁₆ClNO₅S [M+H]⁺ 394.0510, found 394.0519; HPLC (80% acetonitrile in water): t_R = 5.7 min, 98.5%.

4.1.6.7. Ethyl 3-methyl-5-((4-bromophenyl) sulfonamido) benzofuran-2-carboxylate (7g). Yield, 81.7%; a white powder; ¹H NMR (300 MHz, DMSO-*d*₆): δ 10.39 (s, 1H), 7.80 – 7.69 (m, 2H), 7.68 – 7.52 (m, 3H), 7.47 – 7.39 (m, 1H), 7.17 (dd, *J* = 8.9, 2.2 Hz, 1H), 4.33 (q, *J* = 7.1 Hz, 2H), 2.46 (s, 3H), 1.32 (t, *J* = 7.1 Hz, 3H). ¹³C NMR(75 MHz, Chloroform-*d*): δ 159.30, 150.95, 141.21, 138.44, 133.03, 132.31, 128.87, 128.68, 126.75, 124.91, 122.74, 113.65, 112.70, 60.84, 14.08, 8.98. HRMS (ESI): calcd. For C₁₈H₁₆BrNO₅S [M+H]⁺ 438.0005, found 437.9998; HPLC (80% acetonitrile in water): t_R = 4.5 min, 96.8%.

4.1.6.8. Ethyl 5-((3-bromophenyl) sulfonamido) -3-methylbenzofuran-2-carboxylate (7h). Yield, 57%; a white powder; ¹H NMR (300 MHz, DMSO-*d*₆) δ 10.39 (s, 1H), 7.88 – 7.77 (m, 2H), 7.73 – 7.35 (m, 4H), 7.15 (d, *J* = 7.3 Hz, 1H), 4.32 (q, *J* = 7.0 Hz, 2H), 2.45 (s, 3H), 1.31 (t, *J* = 7.0 Hz, 3H); HRMS (ESI): calcd. For C₁₈H₁₆BrNO₅S [M+H]⁺ 438.0005, found 437.9999; HPLC (80% acetonitrile in water): t_R = 6.5 min, 97.8%.

4.1.6.9. Ethyl 5-((2-bromophenyl) sulfonamido) -3-methylbenzofuran-2-carboxylate (7i). Yield, 69%; a white powder; ¹H NMR (300 MHz, DMSO-*d*₆) δ 10.66 (s, 1H), 8.05 (dd, *J* = 7.3, 2.3 Hz, 1H), 7.86 – 7.76 (m, 1H), 7.61 – 7.45 (m, 3H), 7.40 (d, *J* = 2.2 Hz, 1H), 7.23 (dd, *J* = 9.0, 2.3 Hz, 1H), 4.32 (q, *J* = 7.1 Hz, 2H), 2.43 (s, 3H), 1.31 (t, *J* = 7.1 Hz, 3H); HRMS (ESI): Calcd. For C₁₈H₁₆BrNO₅S [M+H]⁺ 438.0005, found 437.9999; HPLC (80% acetonitrile in water): t_R = 5.5 min, 98.6%.

4.1.6.10. Ethyl 3-methyl-5-((4-(trifluoromethyl) phenyl) sulfonamido) benzofuran-2-carboxylate (7j). Yield, 57%; a white powder; ¹H NMR (300 MHz, DMSO-*d*₆) δ 10.53 (s, 1H), 7.92 (brs, 4H), 7.57 (d, *J* = 8.9 Hz, 1H), 7.43 (d, *J* = 1.9 Hz, 1H), 7.17 (dd, *J* = 8.9, 2.1 Hz, 1H), 4.33 (q, *J* = 7.1 Hz, 2H), 2.45 (s, 3H), 1.32 (t, *J* = 7.1 Hz, 3H); HRMS (ESI): calcd. For

$C_{19}H_{16}F_3NO_5S$ $[M+H]^+$ 428.0774, found 428.0761; HPLC (80% acetonitrile in water): $t_R = 2.9$ min, 97.7%.

4.1.6.11. Ethyl 3-methyl-5-((3-(trifluoromethyl) phenyl) sulfonamido) benzofuran-2-carboxylate (7k). Yield, 71%; a white powder; 1H NMR (300 MHz, DMSO- d_6) δ 10.46 (s, 1H), 8.05 – 7.92 (m, 3H), 7.77 (t, $J = 7.7$ Hz, 1H), 7.57 (d, $J = 8.9$ Hz, 1H), 7.41 (d, $J = 2.2$ Hz, 1H), 7.14 (dd, $J = 8.9, 2.3$ Hz, 1H), 4.32 (q, $J = 7.1$ Hz, 2H), 2.44 (s, 3H), 1.31 (t, $J = 7.1$ Hz, 3H); HRMS (ESI): calcd. For $C_{19}H_{16}F_3NO_5S$ $[M+H]^+$ 428.0774, found 428.0770. HPLC (80% acetonitrile in water): $t_R = 6.2$ min, 98.1%.

4.1.6.12. Ethyl 3-methyl-5-((2-(trifluoromethyl) phenyl) sulfonamido) benzofuran-2-carboxylate (7l). Yield, 79%; a white powder; 1H NMR (300 MHz, DMSO- d_6) δ 10.66 (s, 1H), 8.14 – 8.05 (m, 1H), 7.98 (m, 1H), 7.83 (m, 2H), 7.58 (d, $J = 8.91$ Hz, 1H), 7.44 (d, $J = 2.2$ Hz, 1H), 7.22 (dd, $J = 8.9, 2.2$ Hz, 1H), 4.33 (q, $J = 7.1$ Hz, 2H), 2.44 (s, 3H), 1.32 (t, $J = 7.1$ Hz, 3H); HRMS (ESI): calcd. For $C_{19}H_{17}F_3NO_5S$ $[M+H]^+$ 428.0774, found 428.0769; HPLC (80% acetonitrile in water): $t_R = 8.7$ min, 98.2%.

4.1.6.13. Ethyl 3-methyl-5-((4-nitrophenyl) sulfonamido) benzofuran-2-carboxylate (7m). Yield, 60%; a white powder; 1H NMR (300 MHz, DMSO- d_6) δ 10.64 (s, 1H), 8.40 – 8.30 (m, 2H), 8.00 – 7.91 (m, 2H), 7.58 (d, $J = 8.9$ Hz, 1H), 7.46 (d, $J = 2.0$ Hz, 1H), 7.17 (dd, $J = 8.9, 2.2$ Hz, 1H), 4.33 (q, $J = 7.1$ Hz, 2H), 2.45 (s, 3H), 1.32 (t, $J = 7.1$ Hz, 3H); HRMS (ESI): calcd. For $C_{18}H_{16}N_2O_7S$ $[M+H]^+$ 405.0751, found 405.0736; HPLC (80% acetonitrile in water): $t_R = 5.0$ min, 96.6%.

4.1.6.14. Ethyl 3-methyl-5-((3-nitrophenyl) sulfonamido) benzofuran-2-carboxylate (7n). Yield, 57%; a white powder; 1H NMR (300 MHz, DMSO- d_6) δ 10.58 (s, 1H), 8.50 – 8.38 (m, 2H), 8.06 (d, $J = 8.0$ Hz, 1H), 7.81 (t, $J = 8.0$ Hz, 1H), 7.57 (d, $J = 8.8$ Hz, 1H), 7.46 (d, $J = 2.1$ Hz, 1H), 7.16 (dd, $J = 8.6, 2.2$ Hz, 1H), 4.32 (q, $J = 7.1$ Hz, 2H), 2.46 (s, 3H), 1.31 (t, $J = 7.1$ Hz, 3H); HRMS (ESI): calcd. For $C_{18}H_{16}N_2O_7S$ $[M+H]^+$ 405.075, found 405.0766; HPLC (80% acetonitrile in water): $t_R = 5.3$ min, 97.8%.

4.1.6.15. Ethyl 3-methyl-5-((2-nitrophenyl) sulfonamido) benzofuran-2-carboxylate (7o). Yield, 57%; a red powder; 1H NMR (300 MHz, DMSO- d_6) δ 10.76 (s, 1H), 8.01 – 7.90 (m, 2H), 7.89 – 7.72 (m, 2H), 7.61 (dd, $J = 8.9, 1.9$ Hz, 1H), 7.47 (s, 1H), 7.23 (dd, $J = 8.9, 2.2$ Hz, 1H), 4.33 (q, $J = 7.1, 1.9$ Hz, 2H), 2.47 (s, 3H), 1.32 (t, $J = 7.1, 3H$); HRMS (ESI): calcd. For $C_{18}H_{16}N_2O_7S$ $[M+H]^+$ 405.0751, found 405.0758; HPLC (80% acetonitrile in water): $t_R = 5.1$ min, 95.7%.

4.1.6.16. Ethyl 3-methyl-5-((4-tert-butylphenyl) sulfonamido) benzofuran-2-carboxylate (7p). Yield, 68%; a white powder; 1H NMR (300 MHz, DMSO- d_6) δ 10.29 (s, 1H), 7.71 – 7.62 (m, 2H), 7.56 – 7.49 (m, 3H), 7.39 (s, 1H), 7.21 (dd, $J = 8.9, 2.3$ Hz, 1H), 4.32 (q, $J = 7.1$ Hz, 2H), 2.43 (s, 3H), 1.31 (t, $J = 7.1, 3H$), 1.23 (s, 9H); ^{13}C NMR (75 MHz, Chloroform- d): δ 160.29, 150.94, 152.30, 142.00, 135.72, 131.96, 127.71, 127.14, 126.01, 125.47, 123.90, 115.68, 112.76, 61.31, 35.15, 31.00, 14.38, 9.37; HRMS (ESI): calcd. For $C_{22}H_{25}NO_5S$ $[M+H]^+$ 416.1526, found 416.1535; HPLC (80% acetonitrile in water): $t_R = 8.4$ min, 97.3%.

4.1.6.17. Ethyl 3-methyl-5-((3, 4-dimethoxyphenyl) sulfonamido) benzofuran-2-carboxylate (7q). Yield, 90%; a white powder; 1H NMR (300 MHz, DMSO- d_6) δ 10.12 (s, 1H), 7.55 (d, $J = 8.9$ Hz, 1H), 7.44 (d, $J = 2.1$ Hz, 1H), 7.33 – 7.22 (m, 2H), 7.18 (dd, $J = 9.0, 2.2$ Hz, 1H), 7.02 (d, $J = 8.3$ Hz, 1H), 4.33 (q, $J = 7.1$ Hz, 2H), 3.74 (d, $J = 13.1$ Hz, 6H), 2.46 (s, 3H), 1.32 (t, $J = 7.1, 3H$); ^{13}C NMR (75 MHz, Chloroform- d): δ 160.30, 150.74, 152.14, 148.97, 141.91, 132.29, 130.09, 129.61, 125.39, 123.60, 121.40, 115.35, 112.63, 110.31, 109.60, 61.32, 56.10, 56.07, 14.34, 9.37; HRMS (ESI): calcd. For $C_{20}H_{21}NO_7S$ $[M+H]^+$ 420.1111, found 420.1116; HPLC (80% acetonitrile in water): $t_R = 4.6$ min, 94.7%.

4.1.6.18. Ethyl 3-methyl-5-((2, 5-dimethoxyphenyl) sulfonamido) benzofuran-2-carboxylate (7r). Yield, 62%; a white powder; 1H NMR (300 MHz, DMSO- d_6) δ 10.42 (s, 1H), 7.88 (d, $J = 8.9$ Hz, 1H), 7.74 (d, $J = 2.1$ Hz, 1H), 7.62 – 7.57 (m, 2H), 7.45 (d, $J = 1.7$ Hz, 2H), 4.66 (q, $J = 7.1$ Hz, 2H), 4.17 (s, 3H), 4.02 (s, 3H), 2.78 (s, 3H), 1.65 (t, $J = 7.1$ Hz, 3H); HRMS (ESI): calcd. For $C_{20}H_{21}NO_7S$ $[M+H]^+$ 420.1111, found 405.1110; HPLC (80% acetonitrile in water): $t_R = 4.5$ min, 97.7%.

4.1.6.19. Ethyl 3-methyl-5-((naphthalene-2-sulfonamido) benzofuran-2-carboxylate (7s). Yield, 65%; a white powder; 1H NMR (300 MHz, DMSO- d_6) δ 10.42 (s, 1H), 8.41 (d, $J = 1.7$ Hz, 1H), 8.11 (d, $J = 7.2$ Hz, 1H), 8.08 – 7.96 (m, 2H), 7.83 – 7.58 (m, 3H), 7.57 – 7.44 (m, 2H), 7.21 (dd, $J = 8.8, 2.3$ Hz, 1H), 4.33 (q, $J = 7.1$ Hz, 2H), 2.44 (s, 3H), 1.32 (t, $J = 7.1$ Hz, 3H); HRMS (ESI): calcd. For $C_{22}H_{19}NO_5S$ $[M+H]^+$ 410.1057, found 410.1061; HPLC (80% acetonitrile in water): $t_R = 6.3$ min, 98.0%.

4.1.6.20. Ethyl 3-methyl-5-((thiophene-2-sulfonamido) benzofuran-2-carboxylate (7t). Yield, 78%; a yellow powder; 1H NMR (300 MHz, DMSO- d_6) δ 10.42 (s, 1H), 7.87 (dd, $J = 4.96, 1.41$ Hz, 1H), 7.59 (dd, $J = 8.9, 1.9$ Hz, 1H), 7.54 – 7.41 (m, 2H), 7.23 (dd, $J = 8.9, 2.2$ Hz, 1H), 7.14 – 7.07 (m, 1H), 4.34 (q, $J = 7.1$ Hz, 2H), 2.47 (s, 3H), 1.33 (t, $J = 7.1$ Hz, 3H); HRMS (ESI): Calcd. For $C_{16}H_{15}NO_5S_2$ $[M+H]^+$ 366.0464, found 366.0472; HPLC (80% acetonitrile in water): $t_R = 4.8$ min, 98.1%.

4.1.6.21. Ethyl 3-methyl-5-((pyridine-3-sulfonamido) benzofuran-2-carboxylate (7u). Yield, 73%; a pink powder; 1H NMR (300 MHz, DMSO- d_6) δ 10.52 (s, 1H), 8.88 – 8.72 (m, 2H), 8.11–7.96 (m, 1H), 7.63 – 7.52 (m, 2H), 7.45 (d, $J = 2.1$ Hz, 1H), 7.17 (dd, $J = 8.9, 2.2$ Hz, 1H), 4.33 (q, $J = 7.1$ Hz, 2H), 2.46 (s, 3H), 1.32 (t, $J = 7.1$ Hz, 3H); HRMS (ESI): calcd. For $C_{17}H_{16}N_2O_5S$ $[M+H]^+$ 361.0853, found 361.0855; HPLC (80% acetonitrile in water): $t_R = 4.2$ min, 95.5%.

4.2 Biology

4.2.1. Luciferase reporter assays

HIF-1 transactivation activity was determined by transiently transfecting MCF-7 cells with a construct expressing luciferase under the control of three hypoxia response elements (24-mers) from the P_{gk}-1 gene. HRE-luciferase was a gift from Navdeep Chandel (Addgene plasmid # 26731).³⁷ Plasmid DNA was prepared using a commercial kit (TIANGEN, Beijing, China). The empty pGL3 control plasmid and the pRL-SV40 *renilla* luciferase containing plasmid used as controls for transfection efficiency were purchased from Promega (Madison, Wisconsin).

MCF-7 cells in each well of 48-well culture plate were transfected with 0.4 µg plasmid using 1 µL Lipofectamine 2000 Transfection Reagent (Invitrogen, Calif., USA) according to the manufacturer's instructions. 6 h later cells were exposed to hypoxia or normoxia with or without test compounds. After incubation for 24 h, cells were washed twice with ice-cold PBS and lysed with 100 µL of Passive Lysis buffer (Promega) and incubated at room temperature for 10 min. Lysates were centrifuged and supernatants were stored at -80°C until assayed. Luciferase assays were done by pipetting 20 µL of cell lysate into each well of a 96-well plate and analyzed immediately after addition of luciferase reagent (Promega) by Luminoskan Ascent (Thermo Scientific, USA). The data were obtained in triplicates and expressed with the comparison of control.

$$\text{Inhibition rate (\%)} = 1 - [(\text{RLU}_{\text{treated}} - \text{RLU}_{\text{blank}}) / (\text{RLU}_{\text{control}} - \text{RLU}_{\text{blank}})] \times 100\%$$

RLU = relative light unit

4.2.2. MTT assay

The *in vitro* cytotoxicity was determined by MTT assay. The cells (1×10^4 cells/mL) were seeded into 96-well culture plates. After overnight incubation, the cells were treated with various concentrations of compounds or DMSO for 72 h. Then 20.0 µL 3-(4,5-dimethylthiazol-2-yl)-2,5-diphenyl tetrazolium bromide (MTT, Sigma, St. Louis, MO) solution (5 mg/mL in PBS) was added into each well for 4 h at 37°C. Then the solution of MTT was removed, followed by the addition of 150.0 µL DMSO to dissolve the precipitate. The absorbance was measured at 490 nm using Elx800 absorbance microplate reader (BioTek, Vermont, USA) and the OD values were obtained. Cell growth inhibitor y ratio was calculated using the following equation: Inhibitory rate (%) = $[1 - (\text{OD}_{\text{treated}} - \text{OD}_{\text{blank}}) / (\text{OD}_{\text{control}} - \text{OD}_{\text{blank}})] \times 100\%$. The IC₅₀ was then analyzed using GraphPad Prism software.

4.2.3. Western blot analysis

After drug treatment for the specified period, the MCF-7 cells were washed with ice-cold PBS for three times and were harvested by $1 \times$ trypsin. After being centrifuged at 2000 rpm for 5min, the cells were lysed in 80.0 µL of lysis buffer (150.0 mM NaCl, 1% NP-40, 50.0 mM Tris-HCl, pH 7.5, 1mM NaF, EDTA, DTT, Leu, and PMSF) for 1 h. Then cells were centrifuged again at 12000 rpm for 20 min at 4 °C. The supernatant was collected, and the quantification of the whole cell lysates was determined by BCA analysis with Varioskan Flash (Thermo, Waltham, MA) at 567 nm. The lysates were boiled for 5 min in sample loading buffer (5 ×, Beyotime technology) at a ratio of 4:1. The cell lysates were subjected to SDS-PAGE, transferred to PVDF membrane (GE healthcare), and immunoblotted with anti-HIF-1α antibody (ab51608, Abcam). β-actin was used as an internal control. After further incubation with HRP-conjugated secondary antibody, the blots were filmed through the Odyssey infrared imaging System (LI-COR, Lincoln, Nebraska, USA).

4.2.4. Quantitative PCR analysis

Total RNA of MCF-7 cells was isolated using Trizol (Invitrogen). Concentration and purity of RNA samples were determined using NanoDrop 2000 spectrophotometer (Thermo Fisher Scientific). cDNA was reversely transcribed from 1 µg of the total RNA using PrimeScript RT reagent kit (Takara) on a randomprimer. For the quantitative real-time PCR, DNA amplification was carried out using the Fast Start Universal

SYBR Green Master (ROX) (Roche). Primers used for PCR were as follows: human HIF-1α, 5'-TACTAGCTTTGCAGAATGCTC-3' (sense) and 5'-GCCTTGATAGGAGCATTAAAC-3' (antisense); human VEGF, 5'-CCTTGCTGCTCTACCTCCAC-3' (sense) and 5'-CACACAGGATGGCTTGAAGA-3' (antisense); human β-actin, 5'-TGACGTGGACATCCGCAAAG-3' (sense) and 5'-CTGGAAGGTGGACAGCGAGG-3' (antisense). Relative expression level was calculated by the $\Delta\Delta C_T$ method using a StepOne™ Real-Time PCR System (Thermo Fisher Scientific), and normalized with β-actin mRNA level.

4.2.5. VEGF ELISA

3×10^5 cells were seeded onto 6-well plates in serum-free medium containing various concentrations of compound (0, 2.5, 5, 10, 25 and 50 µM) and incubated for 24 h under hypoxic conditions. The conditioned medium was collected, and VEGF levels were determined by VEGF ELISA kit (Neobioscience, Shenzhen, China) according to the manufacturer's protocols. VEGF was expressed as a picogram of VEGF protein per milliliter medium and per 10^5 cells.

4.2.6. Wound healing assay

HUVEC cells were seeded in 6 well plates with a density of 3×10^5 cells/well. After 24 hours, confluent monolayers were gently scratched with a sterile 200 µL tip to create a uniform wound area. After scratching, cells were incubated in fresh media with 2.5, 5, 10, 25, and 50 µM of **7q**. Cell movement and migration into the wound area were examined after 24 hours by Olympus IX51 (Tokyo, Japan) using a 10 × objective. The result was quantified using the ImageJ software (National Institutes of Health).

4.2.7. Capillary-like tube formation

Matrigel (12.5 mg/mL, BD Biosciences, MA, USA) was thawed at 4 °C for overnight, and 50 mL Matrigel was quickly pipetted onto 96-well plate and allowed to solidify for 30 min. HUVECs (1×10^4 cells/well) were seeded on the surface of the matrigel and incubated for 30 min. After adhesion of the cells, the medium was removed and replaced by fresh medium supplemented with various concentrations of **7q**, and incubated for another 24 h under hypoxic condition. The tube formation was photographed with an Olympus IX51 (Tokyo, Japan) using a 10 × objective.

4.2.8. Chicken chorioallantoic membrane (CAM) assay

Anti-angiogenic effect of **7q** on CAM was assayed according to the method described with modification.³¹ Sterilized filter paper disks (5 × 5 mm) that were saturated with 15 µL **7q** (0, 10, 25, and 50 µM) were placed on the CAMs. They were then incubated at 37 °C under normoxia and hypoxia conditions for another 3 days. Then, an appropriate volume of 10% fat emulsion (Sino-Swed Pharmaceutical Corp. Ltd, China) was injected into the embryo chorioallantois for observing the density and length of vessels toward the CAM face. Neovascular zones under the filter paper disks were observed and photographed with a digital camera at × 5 magnification. The number of newly grown vessels was counted on digitalized pictures.

4.2.9. Statistical analysis

All values were expressed as mean ± standard deviation (SD)

from triplicate experiments performed in a parallel manner unless otherwise indicated. Data were analyzed using one-way ANOVA of GraphPad Prism. The level of significance was indicated as * $P < 0.05$, ** $P < 0.01$, and *** $P < 0.001$.

Acknowledgments

This work is supported by 2013ZX09402102-001-005 of the National Major Science and Technology Project of China (Innovation and Development of New Drugs); 2012AA020301 of 863 key program; and the Priority Academic Program Development of Jiangsu Higher Education Institutions.

References and notes

- Darnell, J. E. Transcription factors as targets for cancer therapy. *Nat. Rev. Cancer* **2002**, *2*, 740.
- Semenza, G. L. Hypoxia-inducible factors: mediators of cancer progression and targets for cancer therapy. *Trends Pharmacol. Sci.* **2012**, *33*, 207.
- Semenza, G. L. HIF-1 mediates metabolic responses to intratumoral hypoxia and oncogenic mutations. *J. Clin. Invest.* **2013**, *123*, 3664.
- Nordgren, I. K.; Tavassoli, A. Targeting tumour angiogenesis with small molecule inhibitors of hypoxia inducible factor. *Chem. Soc. Rev.* **2011**, *40*, 4307.
- Tang, C. M.; Yu, J. Hypoxia-inducible factor-1 as a therapeutic target in cancer. *J. Gastroen. Hepatol.* **2013**, *28*, 401.
- Wang, G. L.; Jiang, B. H.; Rue, E. A.; Semenza, G. L. Hypoxia-inducible factor 1 is a basic-helix-loop-helix-PAS heterodimer regulated by cellular O₂ tension. *Proc. Natl. Acad. Sci. U.S.A.* **1995**, *92*, 5510.
- Semenza, G. L. Targeting HIF-1 for cancer therapy. *Nat. Rev. Cancer* **2003**, *3*, 721.
- Jaakkola, P.; Mole, D. R.; Tian, Y. M.; Wilson, M. I.; Gielbert, J.; Gaskell, S. J.; von Kriegsheim, A.; Hebestreit, H. F.; Mukherji, M.; Schofield, C. J.; Maxwell, P. H.; Pugh, C. W.; Ratcliffe, P. J. Targeting of HIF- α to the von Hippel-Lindau ubiquitylation complex by O₂-regulated prolyl hydroxylation. *Science* **2001**, *292*, 468.
- Maxwell, P. H.; Wiesener, M. S.; Chang, G. W.; Clifford, S. C.; Vaux, E. C.; Cockman, M. E.; Wykoff, C. C.; Pugh, C. W.; Maher, E. R.; Ratcliffe, P. J. The tumour suppressor protein VHL targets hypoxia-inducible factors for oxygen-dependent proteolysis. *Nature* **1999**, *399*, 271.
- Fels, D. R.; Koumenis, C. HIF-1 α and p53: the ODD couple? *Trends Biochem. Sci.* **2005**, *30*, 426.
- Hewitson, K. S.; McNeill, L. A.; Riordan, M. V.; Tian, Y. M.; Bullock, A. N.; Welford, R. W.; Elkins, J. M.; Oldham, N. J.; Bhattacharya, S.; Gleadle, J. M.; Ratcliffe, P. J.; Pugh, C. W.; Schofield, C. J. Hypoxia-inducible factor (HIF) asparagine hydroxylase is identical to factor inhibiting HIF (FIH) and is related to the cupin structural family. *J. Biol. Chem.* **2002**, *277*, 26351.
- Freedman, S. J.; Sun, Z. Y.; Poy, F.; Kung, A. L.; Livingston, D. M.; Wagner, G.; Eck, M. J. Structural basis for recruitment of CBP/p300 by hypoxia-inducible factor-1 α . *Proc. Natl. Acad. Sci. U.S.A.* **2002**, *99*, 5367.
- Dames, S. A.; Martinez-Yamout, M.; De Guzman, R. N.; Dyson, H. J.; Wright, P. E. Structural basis for Hif-1 α /CBP recognition in the cellular hypoxic response. *Proc. Natl. Acad. Sci. U.S.A.* **2002**, *99*, 5271.
- Jemal, A.; Siegel, R.; Ward, E.; Hao, Y.; Xu, J.; Thun, M. J. *CA Cancer J Clin* **2009**, *59*, 225.
- Stajner, I. *International Journal of Cancer* **2010**, *126*, 3010.
- Schwab, L. P.; Peacock, D. L.; Majumdar, D.; Ingels, J. F.; Jensen, L. C.; Smith, K. D.; Cushing, R. C.; Seagroves, T. N. Hypoxia-inducible factor 1 α promotes primary tumor growth and tumor-initiating cell activity in breast cancer. *Breast Cancer Res.* **2012**, *14*, R6.
- Cancer Genome Atlas, N. Comprehensive molecular portraits of human breast tumours. *Nature* **2012**, *490*, 61.
- Ward, C.; Langdon, S. P.; Mullen, P.; Harris, A. L.; Harrison, D. J.; Supuran, C. T.; Kunkler, I. H. New strategies for targeting the hypoxic tumour microenvironment in breast cancer. *Cancer Treat Rev* **2013**, *39*, 171.
- Bando, H.; Toi, M.; Kitada, K.; Koike, M. Genes commonly upregulated by hypoxia in human breast cancer cells MCF-7 and MDA-MB-231. *Biomed Pharmacother* **2003**, *57* (8): 333-40.
- Rapisarda, A.; Uranchimeg, B.; Sordet, O.; Pommier, Y.; Shoemaker, R. H.; Melillo, G. Topoisomerase I-mediated inhibition of hypoxia-inducible factor 1: mechanism and therapeutic implications. *Cancer Res.* **2004**, *64*, 1475.
- Shin, D. H.; Chun, Y. S.; Lee, D. S.; Huang, L. E.; Park, J. W. Bortezomib inhibits tumor adaptation to hypoxia by stimulating the FIH-mediated repression of hypoxia-inducible factor-1. *Blood* **2008**, *111*, 3131.
- Yeo, E. J.; Chun, Y. S.; Cho, Y. S.; Kim, J.; Lee, J. C.; Kim, M. S.; Park, J. W. YC-1: a potential anticancer drug targeting hypoxia-inducible factor 1. *J. Natl. Cancer Inst.* **2003**, *95*, 516.
- Koh, M. Y.; Spivak-Kroizman, T.; Venturini, S.; Welsh, S.; Williams, R. R.; Kirkpatrick, D. L.; Powis, G. Molecular mechanisms for the activity of PX-478, an antitumor inhibitor of the hypoxia-inducible factor-1 α . *Mol. Cancer Ther.* **2008**, *7*, 90.
- GlaxoSmith Kline receives approval for hycamtin (topotecan) capsules for the treatment of relapsed small cell lung cancer. www.drugs.com/newdrugs/gsk-receivesapproval-hycamtin-topotecan-capsulesrelapsed-small-cell-lung-cancer-671.html (Accessed 4 May 2012)
- Bross, P. F.; Kane, R.; Farrell, A. T.; Abraham, S.; Benson, K.; Brower, M. E.; Bradley, S.; Gobburu, J. V.; Goheer, A.; Lee, S. L.; Leighton, J.; Liang, C. Y.; Lostritto, R. T.; McGuinn, W. D.; Morse, D. E.; Rahman, A.; Rosario, L. A.; Verbois, S. L.; Williams, G.; Wang, Y. C.; Pazdur, R. Approval summary for Bortezomib for injection in the treatment of multiple myeloma. *Clin. Cancer Res.* **2004**, *10*, 3954.
- Shin, D. H.; Kim, J. H.; Jung, Y. J.; Kim, K. E.; Jeong, J. M.; Chun, Y. S.; Park, J. W. Preclinical evaluation of YC-1, a HIF inhibitor, for the prevention of tumor spreading. *Cancer Lett.* **2007**, *255*, 107.
- Lee, K.; Kim, H. M. A novel approach to cancer therapy using PX-478 as a HIF-1 α inhibitor. *Arch. Pharm. Res.* **2011**, *34*, 1583.
- Terzuoli, E.; Puppo, M.; Rapisarda, A.; Uranchimeg, B.; Cao, L.; Burger, A. M.; Ziche, M.; Melillo, G. *Cancer Res* **2010**, *70*, 6837.
- Zhang, H.; Qian, D. Z.; Tan, Y. S.; Lee, K.; Gao, P.; Ren, Y. R.; Rey, S.; Hammers, H.; Chang, D.; Pili, R.; Dang, C. V.; Liu, J. O.; Semenza, G. L. *Proc Natl Acad Sci U S A* **2008**, *105*, 19579.
- Liu, Y. V.; Baek, J. H.; Zhang, H.; Diez, R.; Cole, R. N.; Semenza, G. L. *Molecular Cell* **2007**, *25*, 207.
- Lee, K.; Qian, D. Z.; Rey, S.; Wei, H.; Liu, J. O.; Semenza, G. L. *Proc Natl Acad Sci U S A* **2009**, *106*, 2353.
- Kaluz, S.; Kaluzova, M.; Stanbridge, E. J. *Mol Cell Biol* **2006**, *26*, 5895.
- Minegishi, H.; Fukushima, S.; Ban, H. S.; Nakamura, H. *ACS Med. Chem. Lett.* **2013**, *4*, 297.
- Uno, M.; Ban, H. S.; Nakamura, H. *Bioorg. Med. Chem. Lett.* **2009**, *19*, 3166.
- Patan, S. *Cancer. Res Treat.* **2004**, *117*, 3.
- Emerling BM, Weinberg F, Liu JL, Mak TW, Chandel NS. *Proc. Natl. Acad. Sci. U.S.A.* **2008**, *105*, 2622.
- Auerbach, R.; Kubai, L.; Knighton, D.; Folkman, J. *Dev Biol.* **1974**, *41*, 391.

Supplementary Material